PNAS
www.pnas.org

Supplementary Information for

Macrophage Angiotensin II type-2 Receptor Triggers Neuropathic Pain

Andrew J. Shepherd, Aaron D. Mickle, Judith P. Golden, Madison R. Mack, Carmen M. Halabi, Annette D. de Kloet, Vijay K. Samineni, Brian S. Kim, Eric G. Krause, Robert W. Gereau IV, and Durga P. Mohapatra

All correspondence should be addressed to Dr. Andrew J. Shepherd (a.shepherd@wustl.edu), and/or Dr. Durga P. Mohapatra (d.p.mohapatra@wustl.edu)

This PDF file includes:

SI Materials and Methods
Figs. S1 to S10
Tables S1 to S2
SI References (68 to 77)

SI Materials and Methods:

Mice

All experiments involving the use of mice and the procedures followed therein were approved by Institutional Animal Studies Committees of Washington University in St. Louis and The University of Iowa, in strict accordance with the *NIH Guide for the Care and Use of Laboratory Animals* (67). Every effort was made to minimize the number of mice used and their suffering. Mice were maintained on a 12:12 light:dark cycle (06:00 to 18:00 hours) with access to food and water *ad libitum.* Unless otherwise stated, 8 to14 week-old male and female mice were used for all experiments. C57BL/6J (Stock No: 000664), FVB/NJ (Stock No: 001800), and *Ma*crophage *F*as-*i*nduced *A*poptosis (MaFIA; stock No: 005070) mice were purchased from Jackson Labs. The MaFIA mouse expresses eGFP and a mutant human FK506 binding protein 1A under the control of the *Csf1r* promoter. This enables selective, inducible depletion of macrophages with administration of a synthetic homodimerizer, AP20187 (44, 45). To induce macrophage (MΦ) depletion, MaFIA mice received 5 daily injections of B/B homodimerizer (AP20187; 2 mg/kg, i.p.) or vehicle (PBS + 10% v/v PEG-400 + 1.7% v/v Tween-80). This treatment regimen is sufficient to reduce Iba1-immunoreactivity in the skin by ~85%, as reported previously. The FVB/NJ-*Agtr2-KO* mouse line was generated by Victor J. Dzau and Richard E. Pratt (20). The AT2R-eGFP reporter mouse line (MMRRC Stock No: 030278-UCD) was generated by Dr. Nathaniel Heintz under the GENSAT project, and backcrossed to C57BL/6J for several generations to yield C57BL/6J-*Agtr2*^{GFP}. All mice were bred and maintained in-house at the Washington University Animal Facility to obtain the required number of mice of specific genotype, gender and age. Specific routes of individual drug injections are mentioned in figures and figure legends. Intrathecal (i.t.) injection was performed by lumbar puncture as described previously (15), using a Hamilton syringe and 30-gauge needles to deliver a volume of 10 µL. Peri-

sciatic administration of PD123319 or vehicle was performed in a volume of 10µl delivered via a 0.3 ml insulin syringe fitted with a 31-gauge needle. The needle was inserted through the *biceps femoris* muscle, adjacent to the nerve injury incision. Mice were continuously monitored post-injection. Experimenters were blinded to mouse sham/surgery conditions, saline/drug injection types, and injection laterality, as well as to mouse sex and genotypes during the conduct of experiments, data recordings and analyses.

Mouse Spared Nerve Injury (SNI) Model of Neuropathy

Mice underwent surgery as part of SNI-induced neuropathy, as described previously in several reports (23, 26, 30, 68). Briefly, mice were anesthetized with isoflurane and an incision was made proximal to the knee, such that the *biceps femoris* muscle could be exposed and separated to access the branches of the sciatic nerve. The common peroneal and tibial nerve branches were ligated with 6-0 silk suture and approximately 1 mm of nerve was removed distally. Following wound closure and administration of post-operative analgesia, mice were monitored for signs of distress and allowed to recover on a heat pad prior to return to the home cage. Sham-operated control mice were operated upon in the same way, except the peroneal and tibial nerve branches of the sciatic nerve were neither ligated nor cut. Subsequent experimentation began on these mice no sooner than post-operative day 5. After sham/surgery the animals were randomly distributed to individual treatment groups.

Behavioral Assessment of Heat, Cold and Mechanical Hypersensitivity

Heat, cold and mechanical sensitivity on mouse hindpaws were assessed as described in previous reports (28-30, 68-70). Animals were acclimated to the testing environment for 30 min on both of the 2 days prior to testing, as well as on every behavioral testing

day. Mice were placed within single-occupancy Plexiglas chambers situated on a glass plate maintained at a constant neutral temperature (30°C). The nociceptive thermal sensitivity of each hindpaw was measured by focusing a beam of light (IITC Life Science) on the plantar surface. The latency to paw withdrawal from the heat source was recorded, and expressed as paw withdrawal latency (PWL). The light intensity was calibrated to elicit baseline PWL values of 10-14 sec. Paw withdrawal latency to a cold stimulus was measured using powdered dry ice packed into a modified 3-mL plastic syringe. The tip of the packed dry ice was applied to the underside of the 5mm glass surface, underneath the plantar surface of the hindpaw. Targeting was achieved using mirrors underneath the testing platform. The mean of two recordings from each hindpaw was used for analysis. The latency cutoff was 20 s, to avoid potential heat/cold-related tissue injury. If a hindpaw was not withdrawn prior to cutoff, a PWL value of 20 s was assigned.

Mechanical sensitivity was measured using 8 von Frey hair filaments of increasing strength (0.04 - 2 g), applied to the extreme lateral edge of the plantar surface of the hindpaw, as described previously (25, 26, 30, 68). Mice were placed on a wire mesh platform covered by a Plexiglas box for 15 min prior to testing. Beginning with the finest filament (0.04 g), each filament was presented to each hindpaw 5 times. The number of paw withdrawal responses was recorded and used for calculating an area under the curve (AUC) value for each hindpaw [scheme shown in Fig. S1A, and (27-30)], which provides a total measure of paw withdrawal response across the entire testing filament range. Based on numerous prior studies showing the effects of SNI induction, and hindpaw injection of CFA and other inflammatory mediators, power analysis was performed to determine the appropriate sample size using the online BioMath software (http://www.biomath.info/). The effective sample size for these experiments was determined as ≥6 per experimental group. For experiments with acute injection of

saline/Ang II ± vehicle/drugs in mice, animals were randomly assigned to individual groups after injections.

Blood Pressure Monitoring

Blood pressure was recorded using a CODA surgical monitor (Kent Scientific) according to the manufacturer's instructions. Mice were habituated to the restraint, placed on a 30°C heat pad, for 10 min on both of two days prior to testing. On the day of testing, after 10 min in the restraint, the occlusion and volume pressure recording cuffs were placed on the tail, and the monitoring was initiated. A minimum of three trials were used for calculating an average systolic and diastolic reading for each animal. All blood pressure monitoring took place between 15:00 and 17:00 hours. Based on numerous prior studies showing the effects of AT receptor antagonists on blood pressure, power analysis was performed to determine the appropriate sample size using the online BioMath software (http://www.biomath.info/). The effective sample size for these experiments was calculated to be ≥5 per experimental group. Mice were randomly assigned to individual groups first after sham/SNI, and subsequently after vehicle/drug injections.

Evans Blue Plasma Extravasation Assay

Assessment of vascular permeability following nerve injury and administration of PD123319 was performed using Evans Blue extravasation (71). 25 µl of 50 mg/ml Evans Blue in sterile saline was injected into the lateral tail vein of mice 60 minutes after i.p. injection of saline or PD123319 (10 mg/kg). Intraplantar injection of saline or 0.5 mg/ml Complete Freund's Adjuvant (CFA) 4h before Evans Blue injection served as a positive control. 15 minutes later, mice were sacrificed and perfused transcardially with chilled 0.1 M phosphate buffer, pH 7.4, for 3 minutes to remove intravascular dye. Plantar

punch biopsies of both hindpaws were placed in 0.1 ml formamide for 96h to extract dye. Absorbance of extracted dye was measured at 620 nm using a Nanodrop spectrophotometer, converted to concentration using a standard curve and normalized to the weight of the biopsy, expressed as µg Evans Blue/mg of tissue. Based on numerous prior studies showing the magnitude of plasma extravasation using Evans Blue injection in mouse hindpaws with painful conditions, power analysis was performed to determine the appropriate sample size using the online BioMath software (http://www.biomath.info/). The effective sample size for these experiments was calculated to be ≥3 per experimental group. Mice were randomly assigned to individual groups first after sham/SNI, and subsequently after vehicle/drug injections.

Angiotensin II Enzyme immunoassay (EIA)

Sciatic nerves and lumbar spinal cord were acutely dissected from animals that had undergone sham or SNI surgery. Plantar punch biopsies were also obtained from mice that had received an intraplantar injection of CFA (0.5 mg/mL) 48 h prior. Tissue samples were homogenized in ice-cold homogenization buffer containing (in mM) 320 sucrose, 5 Na_2HPO_4, 100 NaF, 0.5 phenylmethylsulphonyl fluoride and 1x protease inhibitor cocktail. Triton X-100 was then added to the lysate to a final concentration of 1% (v/v), and allowed to solubilize on a tube rotator for 30 min at 4°C. Following centrifugation at 4°C to pellet debris, total protein concentrations were determined by BCA reagent, and were subsequently analyzed with an angiotensin II enzyme immunoassay (EIA) kit (Sigma-Aldrich), according to the manufacturer's instructions. Tissue samples from 3-4 mice per group were used for this experiment. Results are presented as pg Ang II per 100 µg protein. Experimenters were blinded to mouse sex, surgery and lateralization details during the conduct of these experiments, data recordings and analyses.

Immunohistochemistry

Brain, spinal cord, DRG, and sciatic nerve tissue were harvested from mice as previously described in numerous reports (15, 28, 69, 72, 73). 40 µm-thick fixed frozen sections of mouse brain and spinal cord, and 25 µm-thick sections of mouse DRGs were collected into 0.1 M phosphate buffer (PB). 25 µm-thick sections of mouse sciatic nerve were collected directly onto microscope slides. Tissue sections were incubated with a blocking/permeabilizing solution (10% goat serum in 0.1 M PB + 0.3% Triton X-100) at 4°C for 1 hour, followed by incubation with primary antibodies in blocking solution overnight at 4°C (Table S1). After three 10-min washes in blocking solution, sections were incubated for 3 hours with appropriate secondary antibodies (Table S1). The sections were then washed for 10 min in blocking solution, for 10 min in 0.1 M PB, and finally for 10 min in 0.05 M PB. The sections were then dried on microscope slides and mounted with ProLong Gold anti-fade reagent with DAPI (Molecular Probes). Confocal fluorescence images were captured using a Leica TCS-SPE confocal microscope with a 20X / N.A 0.7 plan apochromat or 40X / N.A. 1.15 apochromatic oil immersion objective. Images are a composite of 11 focal planes in a 20-µm *z*-stack at 2 µm increments. Tissue samples from >3 mice per group for each genotype were used for these experiments. Experimenters were blinded to mouse sex and genotypes, sham/surgery conditions, lateralization, as well as to antibodies used during the conduct of these experiments, image acquisitions and analyses.

ImageJ quantification

Density of Iba1 staining in spinal cord and sciatic nerve was quantified using ImageJ as described previously (74). Threshold RGB intensity was set in a blinded fashion and maintained between images to be compared. Approximately 1.1 mm length of sciatic

nerve and 0.5 mm^2 of spinal cord were captured in each field. The area of the ROI that exhibited fluorescence above threshold was recorded as a percentage value.

Irradiation and Mouse Bone Marrow Transplantation

8-week-old FVB-*Agtr2*-WT recipient mice were irradiated with 950 rads, 6-24 hours prior to receipt of donor bone marrow. Donor marrow was harvested from 8-week-old FVB-*Agtr2*-WT or FVB-*Agtr2*-KO donor mice by centrifugation of femurs and tibias at 6,000xg for 2.5 minutes. Whole bone marrow was then treated with 1 ml Red Blood Cell lysing buffer Hybri-Max (Sigma) for 2 minutes and then filtered through a 70 μm cell strainer. Cells from 2 donors were pooled and injected into 10 recipients in 100 μl PBS by tail vein injection. Recipients were maintained on antibiotic prophylaxis for 1 week following transplantation and allowed to reconstitute for 8 weeks prior to sham/SNI surgery and behavioral testing. Based on prior studies utilizing bone-marrow transplantation experiments in mice, power analysis was performed to determine the appropriate sample size using the online BioMath software (http://www.biomath.info/). The effective sample size for these experiments was calculated to be ≥7 per experimental group. Animals were randomly assigned to individual groups within the genotypes to undergo sham/SNI surgery, and subsequent saline/vehicle/drug injection groups. Experimenters were blinded to mouse sex, genotypes, and irradiation conditions during the conduct of these experiments, image acquisitions and analyses.

Cell Isolation, FACS and Flow Cytometry

Sciatic nerve tissue was finely minced with scissors, digested with collagenase D (1 mg/ml, Roche) for 60 min at 37°C in RPMI medium with 10% FBS (Hyclone) and pressed through a series of strainers to yield single cells as previously described (75). For FACS sorting experiments, $CD11b^+$ cells were separated on FACS-Aria II (BD).

Peripheral mouse blood leukocytes were isolated from whole blood acquired by cardiac puncture. Red blood cells (RBCs) were lysed using 1x RBC lysis buffer (Biolegend) according to the manufacturer's instructions. Following Trypan Blue-based viability assessment and counting, cells were incubated in 1% FBS in DPBS with a panel of lineage-specific antibodies (see table S1), on ice, in darkness for 30 min, before washing. Stained samples were analyzed on a LSR-Fortessa (BD). Dead cells, debris and doublets were excluded on the basis of FSC(A/W) and SSC(A/W), and Zombie Aqua viability dye fluorescence. 20,000 live, singlet, $CD45^+$ events were acquired for each sample. $CD3\varepsilon^+$ $CD19^-$ (T lymphocyte) and $CD3\varepsilon^-$ $CD19^+$ (B lymphocyte) subsets occupied two distinct quadrants, with 'double negative' cells occupying a third. This double negative population was further subdivided into $CD11b^+$ $Ly\text{-}6G^+$ (neutrophils) and $CD11b^+$ $Ly\text{-}6G^-$ (monocyte/MΦ) populations. Data were analyzed using FlowJo 10 software.

RNA Isolation & Quantitative PCR

$CD11b^+$ cells sorted by FACS were collected directly into RLT lysing buffer from the Qiagen RNeasy Plus Micro Kit and processed according to the manufacturer's instructions. Three replicate samples were prepared for each BMT chimera type (*Agtr2*-WT recipient or *Agtr2*-KO recipient), each pooled from 3 individual animals to achieve sufficient cells. mRNA prepared from FVBN/J and *Agtr2*-KO peritoneal macrophages served as positive and negative controls, respectively. 300-500 ng of RNA was transcribed into cDNA using the Superscript III First-Strand Synthesis System for RT-PCR (Invitrogen) according to the manufacturer's instructions. Primers for *Agtr2* and *Gapdh* mRNA (see table S2) were used in qPCR reactions at a final concentration of 500 nM, along with 0.3 µl of cDNA and 12.5 µl of 2x PowerUp SYBR Green Master Mix (Applied Biosystems), with final reaction volume adjusted to 25 µl with molecular biology-

grade water. Reactions were performed in 96-well plates compatible with the StepOnePlus Real-Time PCR System and software (Applied Biosystems), using the 'comparative C_T' ($\Delta\Delta C_T$) method. Following initial denaturation, samples were cycled through denaturation (95°C, 15 s), annealing (50°C, 15 s) and extension (72°C, 60 s) for 40 cycles, followed by melt curve analysis to ascertain specificity of amplification.

Chemicals and Reagents

Losartan (2-Butyl-4-chloro-1-[[2'-(1*H*-tetrazol-5-yl)-[1,1'-biphenyl]-4-yl]methyl]-1*H*-imidazole-5-methanol potassium salt), PD123319 ditrifluoroacetate (1-[[4-(Dimethylamino)-3-methylphenyl]methyl]-5-(diphenylacetyl)-4,5,6,7-tetrahydro-1*H*-imidazo[4,5-*c*]pyridine-6-carboxylic acid ditrifluoroacetate), AMG 9810 ((2*E*)-*N*-(2,3-Dihydro-1,4-benzodioxin-6-yl)-3-[4-(1,1-dimethylethyl)phenyl]-2-propenamide), and A967079 ((1*E*,3*E*)-1-(4-Fluorophenyl)-2-methyl-1-pentene-3-one oxime) were purchased from Tocris – R&D Systems. Complete Freund's Adjuvant and Angiotensin II were purchased from Sigma-Aldrich. The B/B Homodimerizer (AP20187 or B/B-HmD) was purchased from Clontech. All other chemicals used in this study were purchased from Sigma-Aldrich, Bio-Rad, Roche Applied Science, and Thermo Fisher Scientific. We used PD123319 (formerly known as EMA200), a first generation AT2R antagonist. Whereas, the AT2R antagonist (EMA401) used in the phase II clinical trial (8) is the [*S*]-enantiomer of EMA400, a modified EMA200 compound (76, 77). Both PD123319 and EMA401 have >1000-fold selectivity for AT2R over AT1R, and both these antagonists have been shown to attenuate pain hypersensitivity in rodent experimental models with increasing doses and without any visible non-specific effects (76, 77).

Statistical Analysis

Data are presented as mean ± s.e.m. For behavioral experiments, two-way ANOVA with Tukey's multiple comparisons *post hoc* test was performed. $p < 0.05$ in each set of data comparisons was considered statistically significant. Unpaired Student's *t*-test was used for quantification of tissue immunostaining and Ang II EIA experimental results. All analysis was performed using GraphPad Prism 7.0 (GraphPad Software, Inc.).

Supplementary Figures and Figure Legends

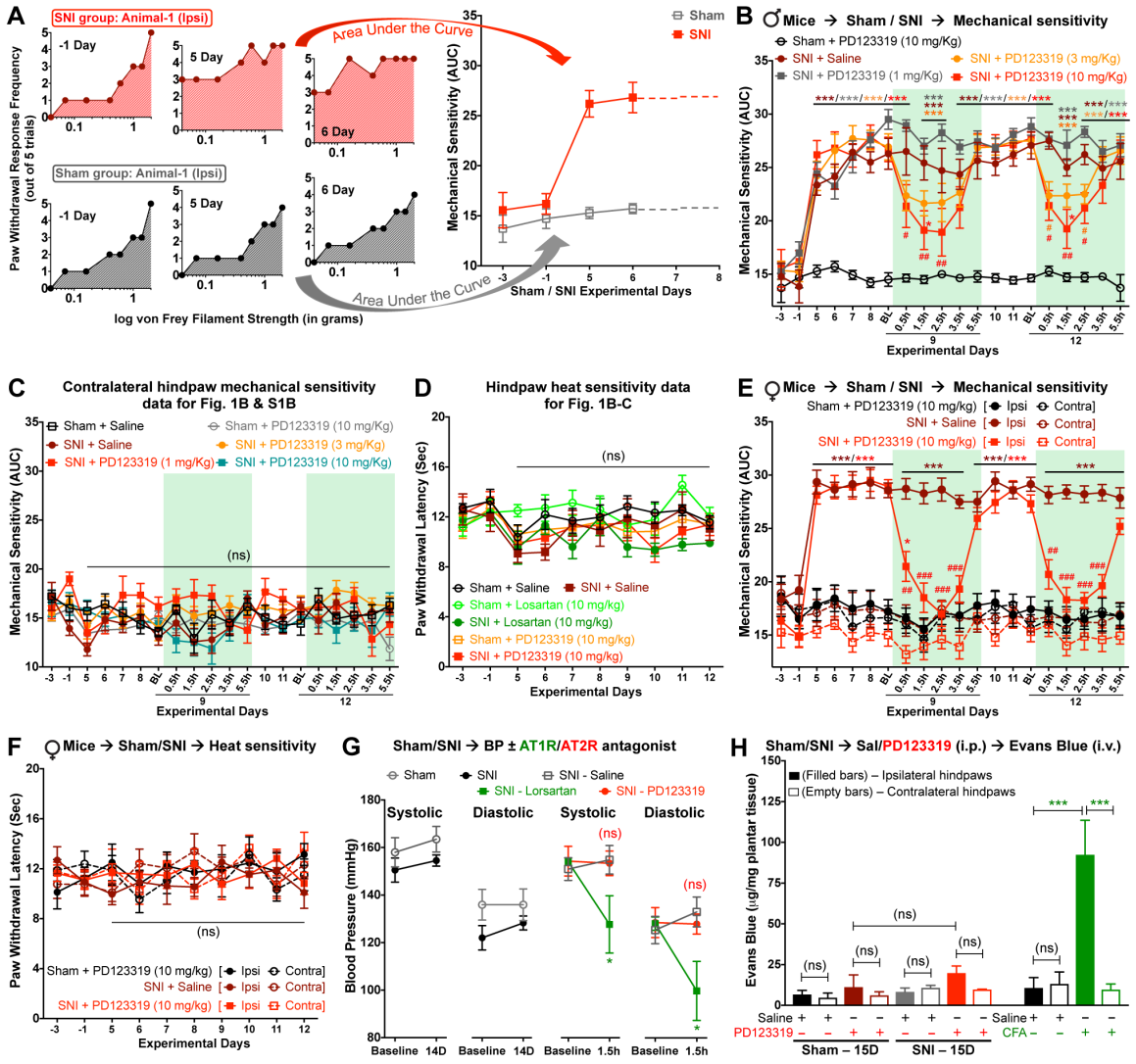

Figure S1: AT2R antagonist dose-dependently attenuates nerve injury-induced mechanical, but not inflammation-induced mechanical or heat hypersensitivity in male and female mice, without any hemodynamic effects. (**A**) Step-by-step depiction of analysis scheme for determination of total mechanical sensitivity (area under the curve or AUC) for paw withdrawal frequencies to increasing strengths of von Frey filaments applied to mouse hindpaws. (**B**) Dose dependent attenuation of SNI-induced mechanical hypersensitivity in male mouse hindpaws by systemic administration (i.p.) of AT2R antagonist PD123319. SNI+saline and SNI+PD123319 (10 mg/kg) group data from Fig. 1B are re-plotted alongside for direct comparison. Mean ± s.e.m. (n=7 or 8 per group); **p*<0.05 and ****p*<0.001, versus sham+PD123319 (10 mg/kg; i.p.) group; $^{\#}p$<0.05 and $^{\#\#}p$<0.01, versus SNI+saline group. (**C**) Mechanical sensitivity data for experimental groups in Fig. 1B and S1B, showing no mechanical hypo- or hypersensitivity in mouse contralateral hindpaws, in response to SNI and/or drug administration. Mean ± s.e.m.

(n=7 or 8 per group). (**D**) No development of heat hypo- or hypersensitivity of mouse ipsilateral hindpaws, in response to SNI; and/or administration of losartan or PD123319 (10 mg/kg for each; i.p.), for experimental groups in Fig. 1B-C. Mean ± s.e.m. (n=7 or 8 per group). (**E**) Attenuation of SNI-induced mechanical hypersensitivity in female mouse hindpaws by systemic administration (i.p.) of AT2R antagonist PD123319. Mean ± s.e.m. (n=7-8 per group); *p<0.05 and ***p<0.001, versus sham+PD123319 (10 mg/kg; i.p.) group; $^{\#\#}p$<0.01 and $^{\#\#\#}p$<0.001, versus SNI+saline group. (**F**) No development of heat hypo- or hypersensitivity in female mouse ipsilateral hindpaws, in response to SNI; or administration of PD123319 (10 mg/kg; i.p.), for experimental groups in Fig. S1E. Mean ± s.e.m. (n=7 or 8 per group). (**G**) No significant alteration in systolic and diastolic blood pressure can be observed in mice subjected to SNI (14 days post-surgery), as compared to sham-operated mice. Systemic administration of PD123319 (10 mg/kg; i.p.; 14 days post-SNI) does not significantly change systolic and diastolic blood pressure (1.5 h post-injection). However, systemic administration of losartan (10 mg/kg; i.p.; 14 days post-sham/SNI) significantly decreases both systolic and diastolic blood pressure, utilized as a positive control. Mean ± s.e.m. (n=≥5 each); *p<0.01 and not significant (ns), versus respective SNI – saline groups. (**H**) No significant change in plantar extravasation of Evans Blue dye is observed 1 h following saline or PD123319 (10 mg/kg; i.p.) in sham or SNI mice (15 days post-surgery). The filled bars indicate ipsilateral hindpaws and the empty bars indicate contralateral hindpaws. Significant dye extravasation was detected 4 h after injection of CFA (10 µl of 1 mg/ml; as positive control). Mean ± s.e.m. (n=3 each); ***p<0.001 CFA-ipsi versus saline-ipsi and CFA-contra. Rectangular boxes in panels B, C and E denote post-drug administration time points for behavioral assessment.

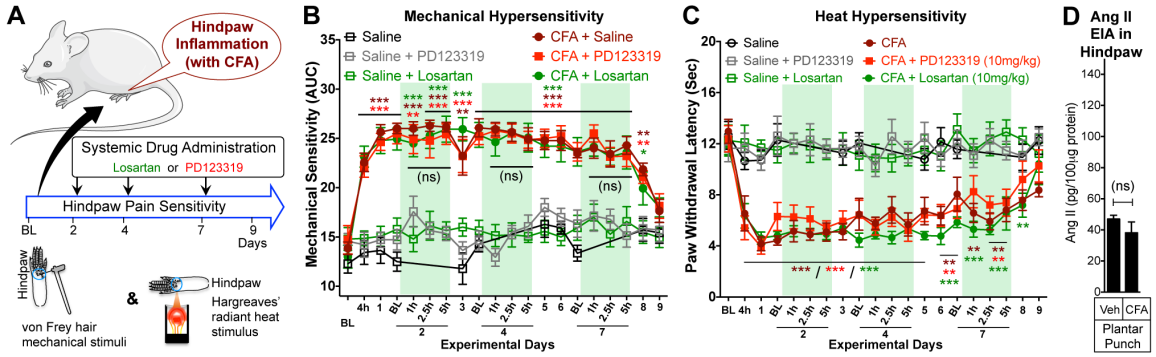

Figure S2: AT2R antagonist does not attenuate inflammation-induced mechanical or heat hypersensitivity in mice.

(**A**) Experimental scheme to test the role of AT1R and AT2R antagonists on hindpaw mechanical and heat hypersensitivity induced by inflammation with CFA injection (10 µl of 1 mg/ml). Antagonists for both AT1R (losartan, 10 mg/kg; i.p.) and AT2R (PD123319, 10 mg/kg; i.p.) failed to attenuate CFA-induced hindpaw mechanical (**B**) and heat (**C**) hypersensitivity. Mean ± s.e.m. (n=7 per group); *p<0.05, **p<0.01 and ***p<0.001 versus respective baseline and saline-injected group time points; not significant (ns) for CFA + PD123319 and CFA + Losartan groups versus respective CFA + Saline group time points. (**D**) CFA injection (10 µl of 1 mg/ml) did not increase local Ang II levels in injected hindpaw plantar region (2 days post-injection), as quantified by EIA. Mean ± s.e.m. (n=3 each); not significant (ns), versus vehicle-injected hindpaw plantar punch group. Rectangular boxes in panels B and C denote post-drug administration time points for behavioral assessment.

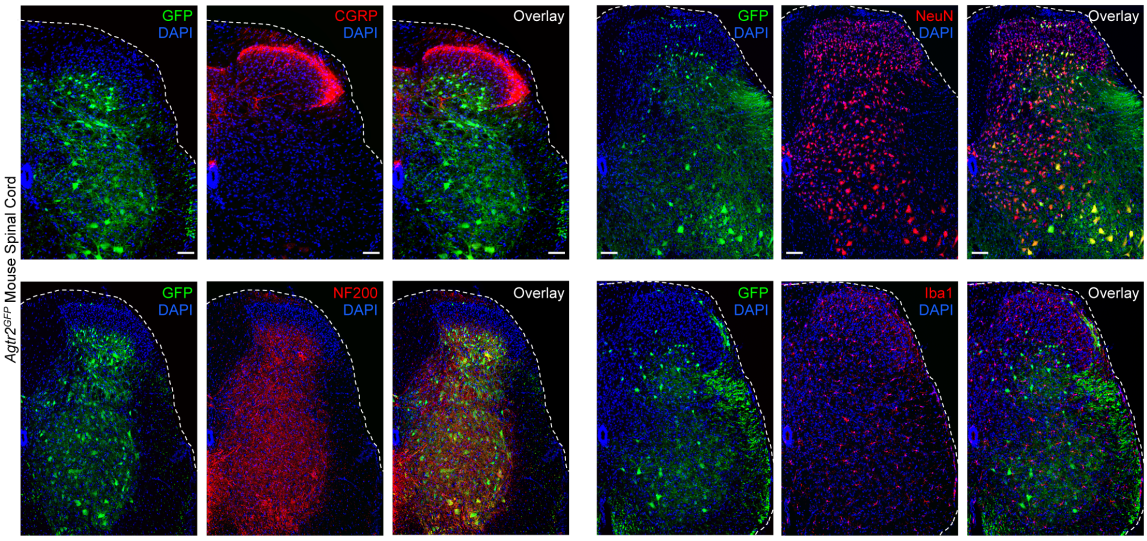

Figure S3: AT2R is expressed in deeper laminae dorsal horn and ventral horn neurons in the spinal cord. GFP immunoreactivity (green) is observed in the spinal cord of *Agtr2*^{GFP} mice. GFP signal is absent in the superficial laminae of the dorsal horn, where central terminals of CGRP-expressing sensory nerve fibers are present (red; upper left). GFP signal in the deep dorsal and ventral horn co-localizes with the neuronal markers NeuN (upper right; red) and NF200 (lower left, red), but not the microglial marker Iba1 (lower right, red). DAPI: blue; scale bar: 50 µm.

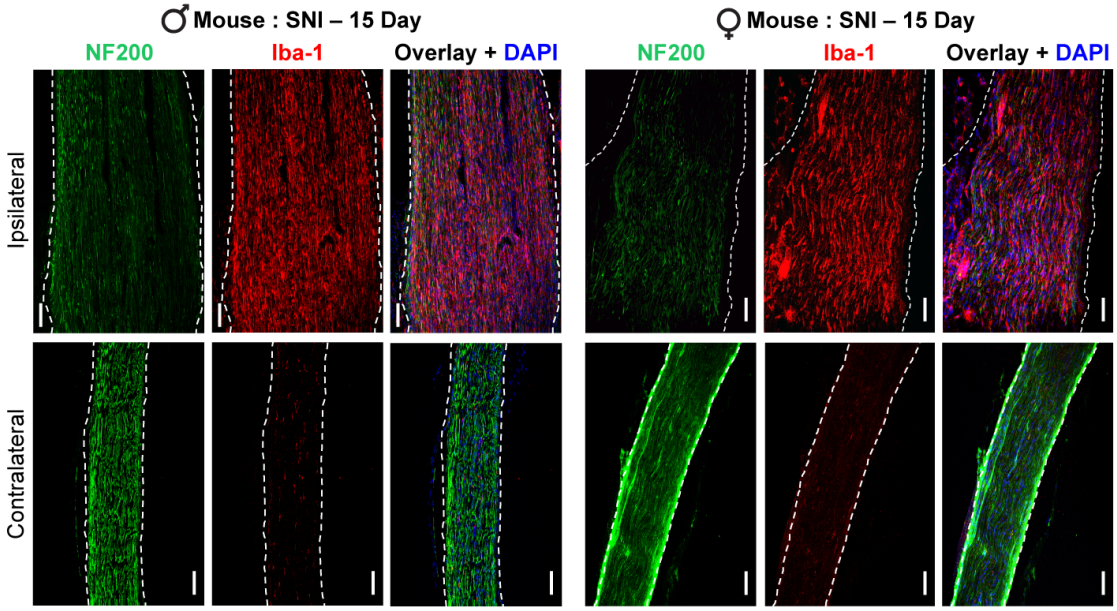

Figure S4: No sex differences in sciatic nerve macrophage (MΦ) infiltration can be observed following SNI. Elevated Iba1-positive immunoreactivity (red) is observed within the ipsilateral, but not contralateral sciatic nerves of both male (left) and female (right) C57BL/6J mice, 15 days post SNI surgery. NF200: green; DAPI: blue; Scale: 200 µm.

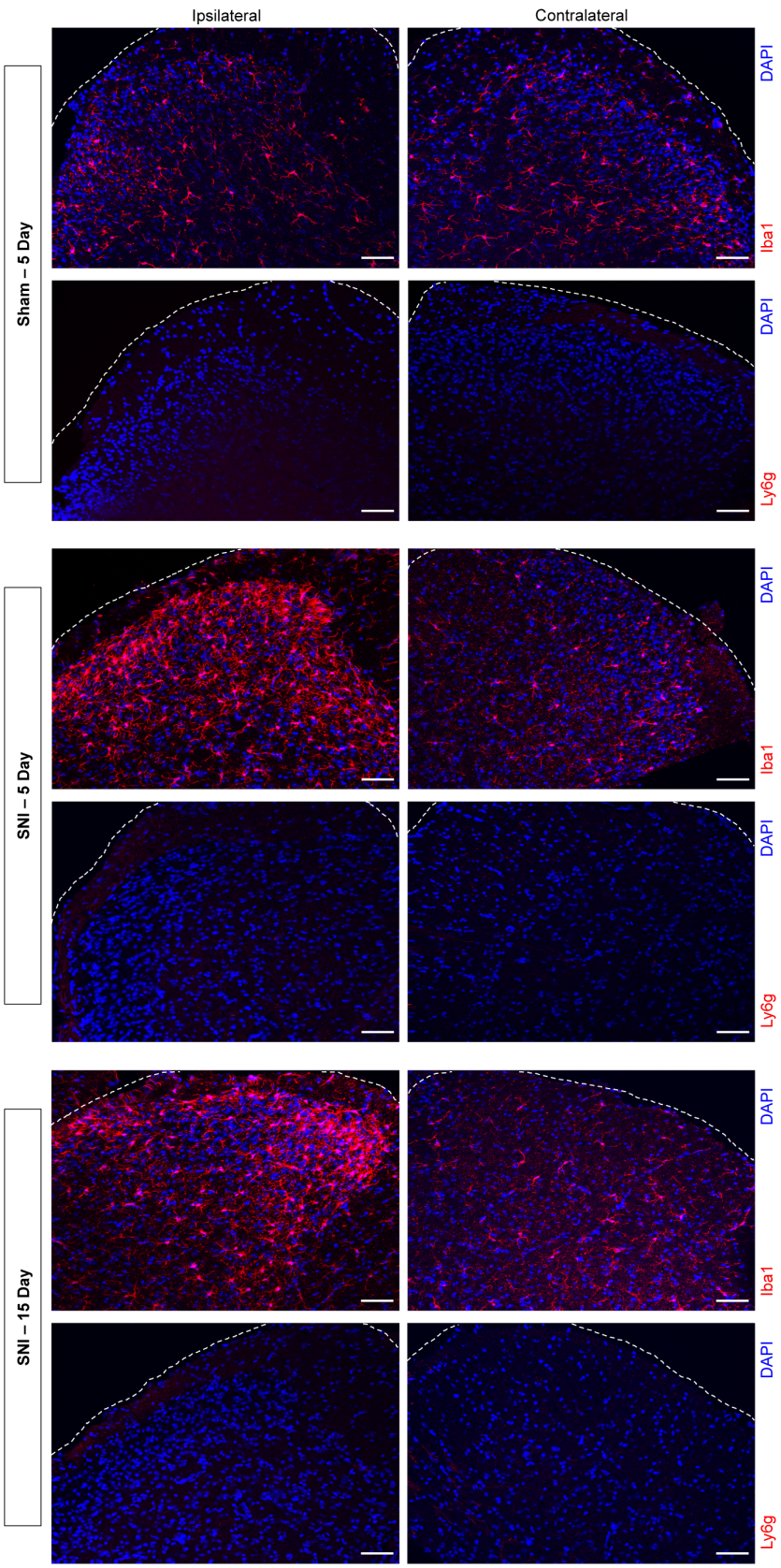
Ipsilateral
Contralateral
Sham – 5 Day
SNI – 5 Day
SNI – 15 Day
DAPI
Iba1
Ly6g

Figure S5: Elevated microglia density can be observed in the ipsilateral spinal cord dorsal horn of mice following SNI. SNI induces increased Iba1 immunoreactivity compared to sham controls in ipsilateral spinal cord dorsal horn (upper rows) at 5 and 15 days post-surgery, without any apparent Ly6g staining (lower rows). DAPI: blue; scale: 50 μm.

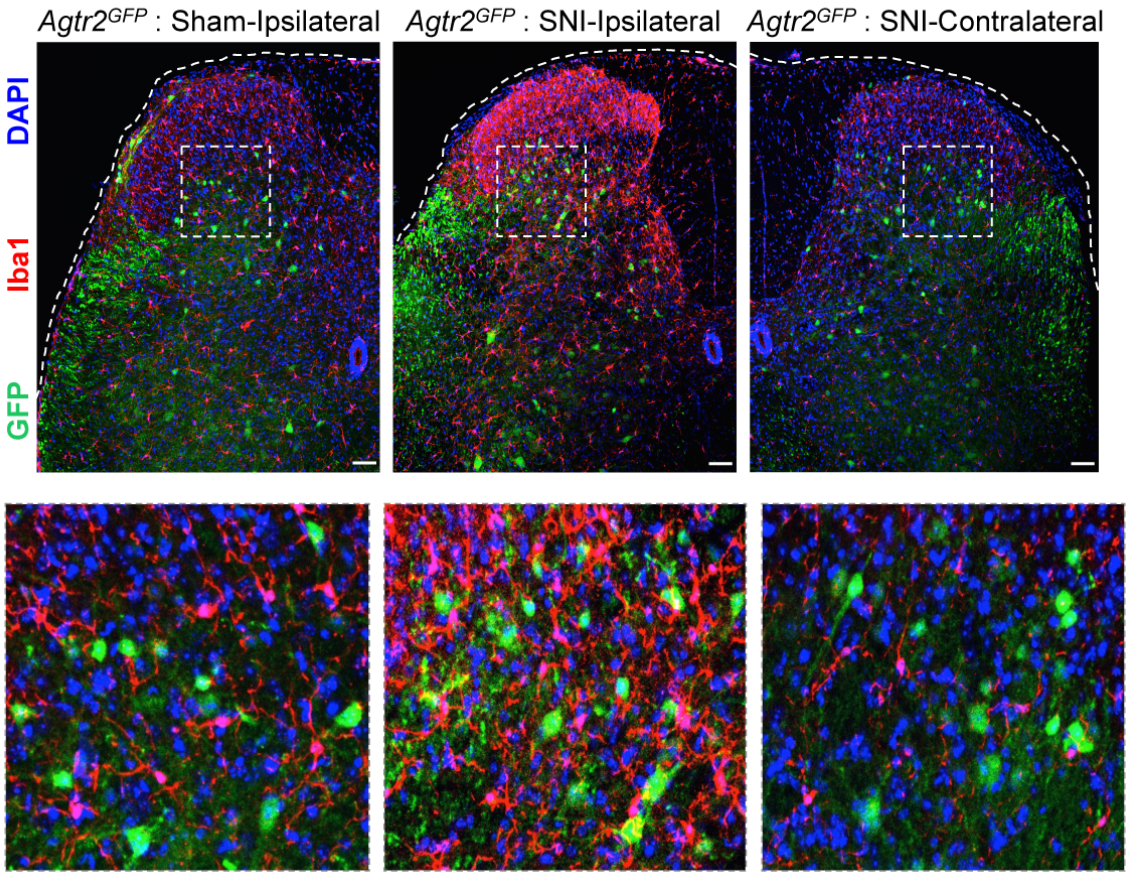

Figure S6: AT2R expression is not detected in spinal cord dorsal horn microglia following SNI. *Agtr2*^{GFP} reporter mouse spinal cord shows no overlap between GFP (green) and Iba1 (red) in the ipsilateral dorsal horns following sham and SNI surgery (10 days post-surgery; left and middle), or in the contralateral dorsal horn of SNI mice (right). DAPI: blue; scale: 50 µm. The bottom row images depict the magnified views of selected rectangular box in the respective top row images.

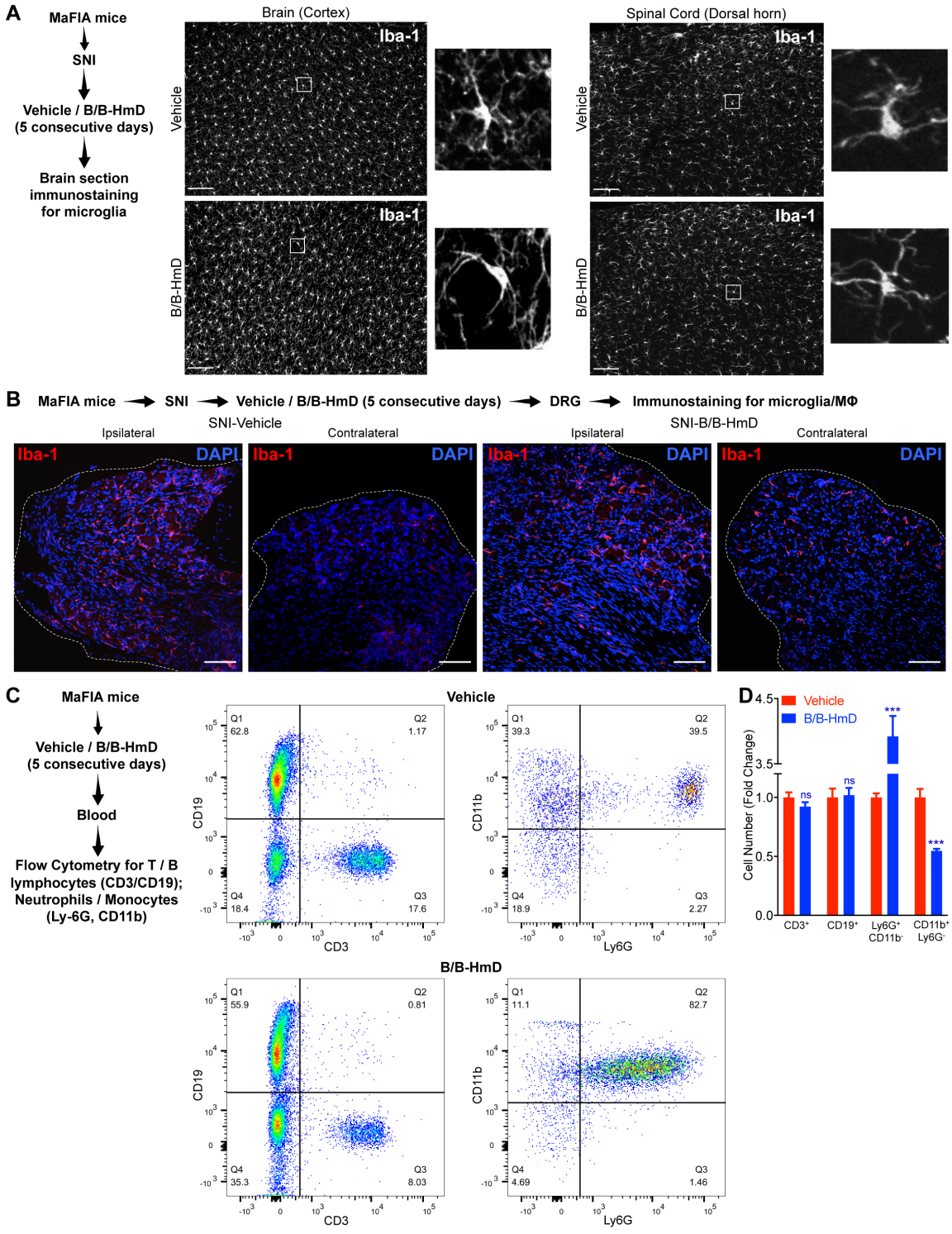

Figure S7: Selective chemogenetic depletion of peripheral macrophages (MΦs), but not lymphocytes/neutrophils or brain/spinal cord/DRG microglia/MΦs, in MaFIA mice. (A) Chemogenetic depletion of MΦs in MaFIA mice with administration of the designer drug B/B-HmD (2 mg/kg/day for 5 days) did not alter microglia/MΦ density in the brain and spinal cord, as shown by confocal microscopic images of Iba-1

immunoreactivity in the brain cortical region. Images on the right are a magnified view of the marked box in respective images. Scale bar: 200 μm. (B) SNI induces elevated Iba-1 immunoreactivity in the ipsilateral DRG, which persists in B/B-HmD-treated animals, at 11 days post-injury. Scale bar: 50 μm. (C) Administration of vehicle to MaFIA mice (~0.1ml/day for 5 days, top row) does not affect blood T- or B-lymphocyte populations; neutrophil and monocyte/MΦ populations also appear normal. Chemogenetic depletion of MΦs in MaFIA mice with administration of the designer drug B/B-HmD (2 mg/kg/day for 5 days) does not significantly affect blood T- or B-lymphocyte numbers (bottom row); however, significant loss of monocytes is accompanied by neutrophilia in these mice. Fold-change in cell numbers is quantified in panel D. Mean ± s.e.m. (n=4 per group). ***p<0.001 and not significant (ns), versus respective vehicle-treated groups.

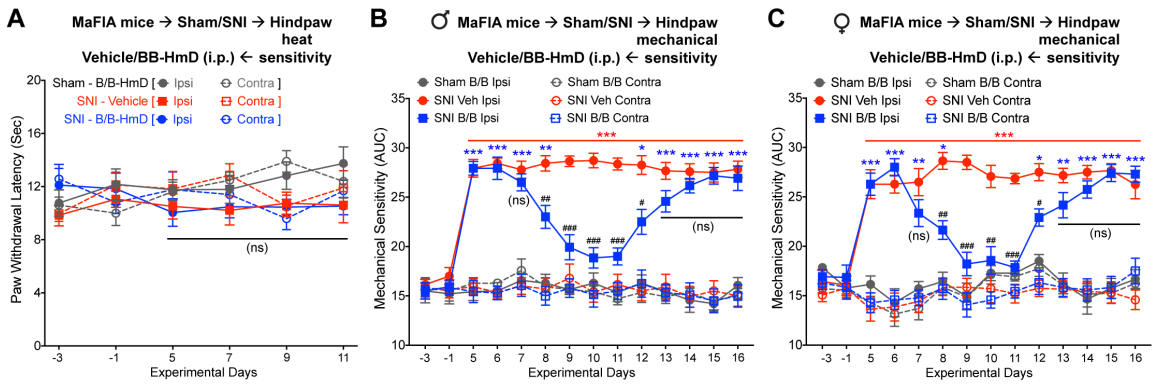

Figure S8: Depletion of peripheral macrophages (MΦs) attenuates hindpaw mechanical hypersensitivity in male and female MaFIA mice, without any influence on heat sensitivity. (A) SNI does not lead to the development of heat hypo- or hypersensitivity in MaFIA mice upon chemogenetic depletion of peripheral MΦs with B/B-HmD (2 mg/kg/day for 5 days, starting 6 days post-SNI). Mean ± s.e.m. (n=8 per group); not significant (ns) versus respective baselines (-1) and respective time points in sham-B/B-HmD and SNI-B/B-HmD groups. (B) SNI leads to the development of mechanical hypersensitivity in male MaFIA mice, which is attenuated upon chemogenetic depletion of peripheral MΦs with B/B-HmD (2 mg/kg/day for 5 days, starting 6 days post-SNI). Mean ± s.e.m. (n=7 per group). *p<0.05 **p<0.01 and ***p<0.001, versus sham+BB-HmD-ipsilateral group; $^{\#}p$<0.05, $^{\#\#}p$<0.01, $^{\#\#\#}p$<0.001 and not significant (ns), versus SNI+vehicle ipsilateral group. (C) SNI leads to the development of mechanical hypersensitivity in female MaFIA mice, which is attenuated upon chemogenetic depletion of peripheral MΦs with B/B-HmD (2 mg/kg/day for 5 days, starting 6 days post-SNI). Mean ± s.e.m. (n=7 per group). *p<0.05 **p<0.01 and ***p<0.001, versus sham+BB-HmD-ipsilateral group; $^{\#}p$<0.05, $^{\#\#}p$<0.01, $^{\#\#\#}p$<0.001 and not significant (ns) versus SNI+vehicle ipsilateral group.

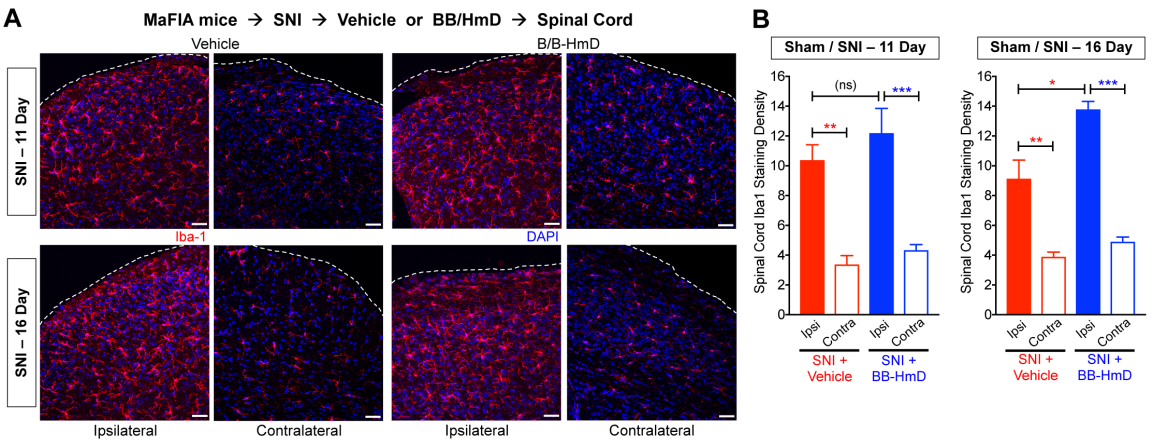

Figure S9: Chemogenetic depletion of peripheral macrophages (MΦs) in MaFIA mice did not influence nerve injury/neuropathy-induced enhancement of spinal cord microglia density.

(A) Representative confocal microscopic images of spinal cord dorsal horn from sham/SNI mice treated with vehicle/BB-HmD, showing increased microglial proliferation/ density (Iba-1: red, DAPI: blue; scale bar: 50 μm). (B) Quantification of images depicted in panel A. Mean ± s.e.m. (n= 2 sections each from 4 mice/group), *p<0.05 **p<0.01, ***p<0.001, and 'ns' denotes not significant, versus respective ipsilateral/contralateral comparison groups/time points.

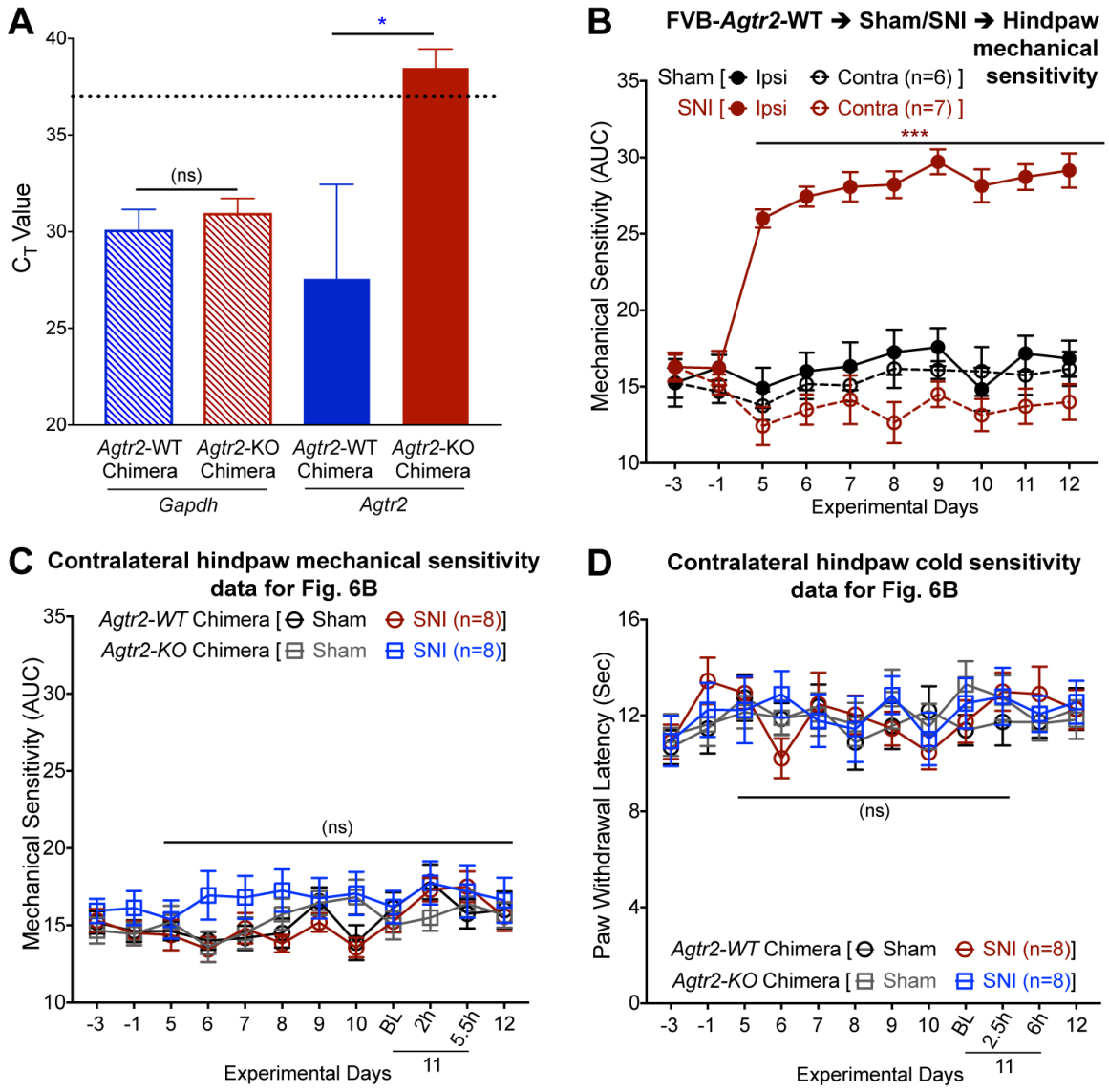

Figure S10: SNI induces hindpaw mechanical hypersensitivity in FVB-*Agtr2*-WT mice, and no alteration in mechanical and cold hypersensitivity of contralateral hindpaws of *Agtr2*-WT or *Agtr2*-KO chimeras. (A) qPCR-based validation of Agtr2 transcript in infiltrating macrophages from injured sciatic nerves of *Agtr2*-WT and *Agtr2*-KO BMT chimeras. Dotted line represents mean negative control C_T value (37.1°C). Mean ± s.e.m. *p<0.05 and not significant (ns) versus respective Agtr2-WT chimera groups. (B) SNI induction leads to long-lasting mechanical hypersensitivity in the hindpaws of FVB-*Agtr2*-WT mice, similar to observations in C57BL/6J mice. Mean ± s.e.m. ***p<0.001, versus SNI-ipsi baseline (-1) and respective time points in sham-ipsi group. (C) Mechanical sensitivity data for experimental groups in Fig. 6B, showing no mechanical hypo- or hypersensitivity in mouse contralateral hindpaws, in response to SNI and/or PD123319 (10 mg/kg; i.p.) administration. (D) Cold sensitivity data for experimental groups in Fig. 6B, showing no cold hypo- or hypersensitivity in mouse

contralateral hindpaws, in response to SNI and/or PD123319 (10 mg/kg; i.p.) administration. Mean ± s.e.m. for panels C-D; not significant (ns) versus SNI-ipsi baselines (-1) and respective time points in sham-ipsi groups.

Table S1. Antibodies used in this study.

Antigen	Antibody species / type	Dilution	Vendor	Cat. #
Primary				
Iba1	Rabbit polyclonal IgG	1:500	Wako Chemicals USA	019-19741
Ly6g	Rat monoclonal IgG2b	1:200	Abcam	ab25377
F4/80	Rat monoclonal IgG2b	1:250	ThermoFisher Scientific	MA5-16632
NF200	Mouse monoclonal IgG1	1:250	Sigma-Aldrich	N0142
CGRP	Mouse monoclonal IgG1	1:250	Sigma-Aldrich	C7113
NeuN	Mouse monoclonal IgG1	1:100	EMD Millipore	MAB377
GFP	Goat polyclonal, FITC	1:250	Abcam	ab6662
Flow Cytometry				
CD45	Rat monoclonal IgG2b, PE	1.25 µl / 10^6 cells / 0.1 mL	BioLegend	147711
CD3ε	Syrian Hamster anti-mouse, APC	1.25µl / 10^6 cells / 0.1 mL	BioLegend	152305
CD19	Rat monoclonal IgG2a, Pacific Blue	0.5 µl / 10^6 cells / 0.1 mL	BioLegend	115526
Ly-6G	Rat monoclonal IgG2a, Brilliant Violet 605	1.25 µl / 10^6 cells / 0.1 mL	BioLegend	127639
CD11b	Rat monoclonal IgG2b, PE/Cy7	1.25 µl / 10^6 cells / 0.1 mL	BioLegend	101215
Secondary				
Mouse IgG1-Alexa fluor 488	Goat polyclonal IgG	1:1000	Molecular Probes	A21121
Rat IgG-Alexa fluor 568				A11077
Rabbit IgG-Alexa fluor 488				A11008
Rabbit IgG-Alexa fluor 555				A21428
Goat IgG-Alexa fluor 488	Donkey polyclonal IgG			A11055
Goat IgG-Alexa fluor 555				A21432
Rabbit IgG-Alexa fluor 488				A21206
Rabbit IgG-Alexa fluor 555				A31572

Table S2. Quantitative RT-PCR Primers.

Species & Gene	Primer sets	Annealing Temp. (°C)	Amplicon size (bp)
Mouse *Agtr2*	fwd – 5' CTGCTGGGATTGCCTTAATG 3'	53.5	149
	rev – 5' CATCTTCAGGACTTGGTCAC 3'		
Mouse *Gapdh*	fwd – 5' TGATGACATCAAGAAGGTGGTGAAG 3'	56.7	240
	rev – 5' TCCTTGGAGGCCATGTAGG 3'		

SI References

68. Shepherd AJ, Cloud ME, Cao Y-Q, & Mohapatra DP (2018) Deficits in Burrowing Behaviors are Associated with Mouse Models of Neuropathic but not Inflammatory Pain or Migraine. *Front Behav Neurosci* 12:124.
69. Loo L*, et al.* (2012) The C-type natriuretic peptide induces thermal hyperalgesia through a noncanonical Gbetagamma-dependent modulation of TRPV1 channel. *J Neurosci* 32(35):11942-11955.
70. Brenner DS, Golden JP, & Gereau RWt (2012) A novel behavioral assay for measuring cold sensation in mice. *PLoS ONE* 7(6):e39765.
71. Martin Y, Avendaño C, Piedras MJ, & A. K (2010) Evaluation of Evans blue extravasation as a measure of peripheral inflammation. *Protocol Exchange* 10.1038/protex.2010.209.
72. Shepherd AJ, Loo L, Gupte RP, Mickle AD, & Mohapatra DP (2012) Distinct modifications in Kv2.1 channel via chemokine receptor CXCR4 regulate neuronal survival-death dynamics. *J Neurosci* 32(49):17725-17739.
73. Shepherd AJ & Mohapatra DP (2012) Tissue preparation and immunostaining of mouse sensory nerve fibers innervating skin and limb bones. *J Vis Exp : JoVE* (59):e3485.
74. Jensen EC (2013) Quantitative analysis of histological staining and fluorescence using ImageJ. *Anat Rec* 296(3):378-381.
75. Costa ML*, et al.* (2017) Two Distinct Myeloid Subsets at the Term Human Fetal-Maternal Interface. *Front Immunol* 8:1357.
76. Blankley CJ*, et al.* (1991) Synthesis and structure-activity relationships of a novel series of non-peptide angiotensin II receptor binding inhibitors specific for the AT2 subtype. *J Med Chem* 34(11):3248-3260.

77. Smith MT, Wyse BD, & Edwards SR (2013) Small molecule angiotensin II type 2 receptor (AT(2)R) antagonists as novel analgesics for neuropathic pain: comparative pharmacokinetics, radioligand binding, and efficacy in rats. *Pain Med* 14(5):692-705.